

Amorphization and Structural Relaxation Processes in Ion Implanted Si

T. Motooka, F. Kobayashi, Y. Hiroyama, and T. Tokuyama

*Institute of Applied Physics
University of Tsukuba, Tsukuba, Ibaraki 305, Japan*

Amorphization processes in Si⁺, P⁺, Ge⁺, and As⁺ ion implanted Si as well as structural relaxation of amorphous Si (a-Si) during low-temperature (200-450°C) annealing have been investigated using Raman spectroscopy. Based on the analysis of bond angle deviation $\Delta\theta$ derived from the a-Si TO peak width, we have proposed that (1) amorphization is controlled by ion-beam-induced divacancy concentration and (2) due to dissociation of microvoids in the a-Si layers, $\Delta\theta$ does not decrease monotonically but shows an increase after the initial decrease during isothermal annealing.

1. INTRODUCTION

Ion implantation is a key processing technique in microelectronics device fabrication for controlled doping of Si. As device sizes are decreased, it is increasingly important to understand microscopic structural changes in the Si lattice due to the ion-beam-induced damage and thermal annealing after implantation. Previously, we have studied the dose and substrate temperature effects on amorphization processes in self-ion implanted Si using Raman spectroscopy, Rutherford backscattering spectroscopy, and cross-sectional transmission electron microscopy (TEM).^{1,2} We have proposed that during a precursor stage to amorphization the crystal Si (c-Si) lattice is softened.¹ and an accumulation of small defects induces amorphization at low substrate temperature, while at higher temperatures larger defect complexes are formed and an accumulation of them gives rise to defected amorphous Si (a-Si).²

In this paper, we investigate the effects of ion species on amorphization as well as structural relaxation of a-Si during low temperature (200-450°C) annealing based on Raman spectroscopy measurements combined with computer simulations for the analysis of initial defect distribution generated by ion bombardment.

2. EXPERIMENTAL PROCEDURE

Si⁺, P⁺, Ge⁺, and As⁺ ion implantations were carried out at room temperature in optically flat Czochralski-grown p-type Si(100) substrates with a resistivity of 6-8 Ω -cm. The substrates were oriented 5° off-normal to the incident ion beam for suppression of channeling effects. The ion energies were 100 keV for Si and P, and 175 keV for Ge and As. The ion doses were varied from 0.2 to 1.5 $\times 10^{15}$ cm⁻² for both Si and P, from 0.4 to 2.8 $\times 10^{14}$ cm⁻² for both Ge and As. The current densities were kept less than

1 μ A/cm² to prevent beam heating of the samples.

For the investigation of structural relaxation processes, completely amorphized samples were prepared by implanting 150 keV Si⁺ with a dose of 5 $\times 10^{15}$ cm⁻² at room temperature. Isothermal furnace annealing was performed at 200, 250, 300, and 450 °C for up to 6 hours in dry N₂ ambient.

Raman measurements were carried out at room temperature using a Spex Triplemate 1877. A 120 mW argon-ion laser beam tuned to 488 nm was grazing incident on the sample surfaces with a beam diameter of ~100 μ m and scattered light was observed in the direction normal to the surface through a f/1 lens. Scattered light was first introduced into a zero-dispersion double monochromator to suppress stray light and then dispersed in a f=600 mm single-monochromator with a 1800 l/mm grating. The optical signal was detected by a photomultiplier and processed by a SPEX DM 3000 photon counting system. The monochromator scanning step was 1 cm⁻¹ with a 10 cm⁻¹ spectral slit width and the integration time was 5 seconds for each step.

3. RESULTS AND DISCUSSIONS

Figure 1 shows typical Raman spectra of the 100 keV Si⁺ ion implanted samples with various doses along with a reference spectrum from undamaged c-Si. Similar spectra were obtained in the P⁺, Ge⁺, and As⁺ implanted samples. The sharp c-Si Raman peak at 521 cm⁻¹ is due to the triply degenerate k=0 transverse optical (TO) phonon modes. A broad peak centered at ~300 cm⁻¹ can be attributed to two-phonon transitions³ composed of various combinations of the transverse acoustic (TA) phonon modes. As the dose is increased, since the k-conservation rule for the Raman transition is relaxed due to ion-induced defects, the c-Si peaks corresponding to one- and two-phonon transitions decrease and the Raman spectrum

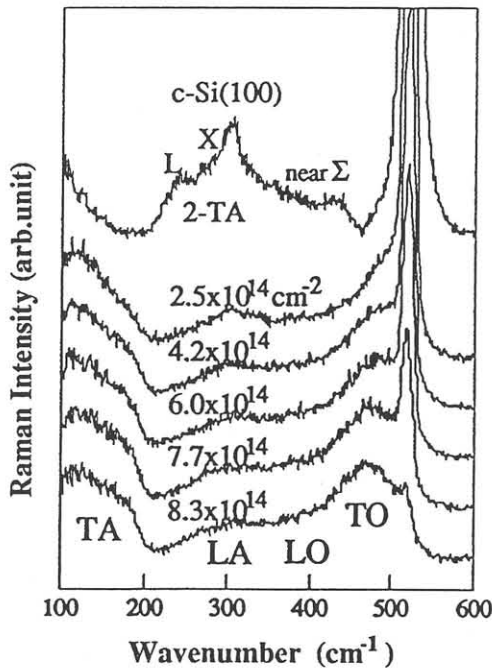


Fig.1 Typical Raman spectra from the 100 keV Si⁺ implanted samples with various implantation doses. The spectrum from undamaged c-Si(100) is also shown for reference.

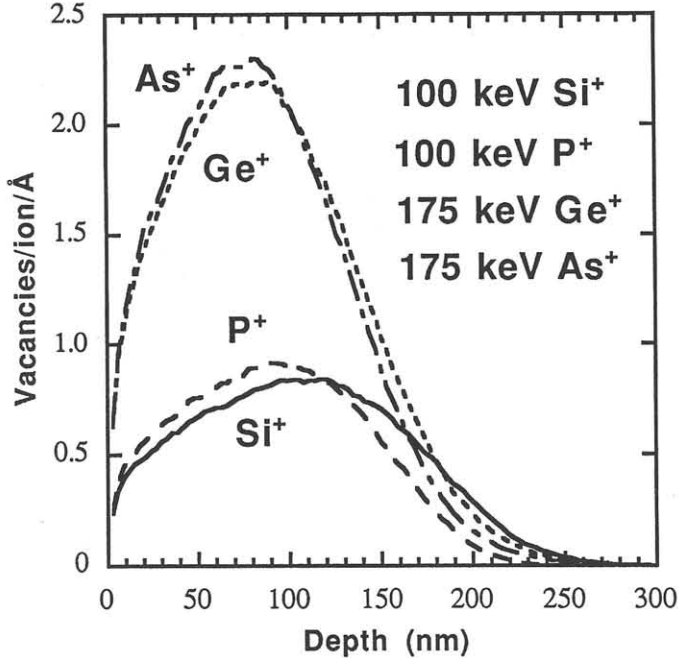


Fig.2 Monte Carlo simulations results for the numbers of vacancies created by an ion per Å. The implantation energies are 100 keV for both Si and P, and 175 keV for both Ge and As.

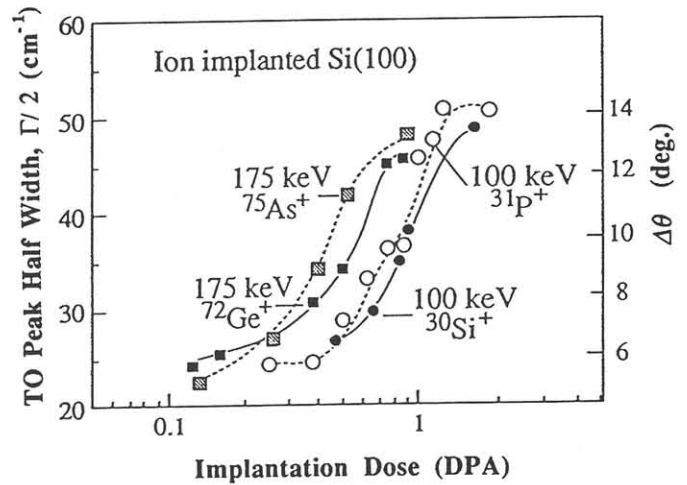


Fig. 3 TO peak half width $\Gamma/2$ and bond angle deviations $\Delta\theta$ in Si⁺, P⁺, Ge⁺, and As⁺ implanted samples as a function of implantation dose scaled by DPA.

changes to that of a-Si which resembles the phonon density of states including the longitudinal optical and acoustic (LO and LA) modes in addition to the TO and TA modes described above.

Beeman et al. proposed the following linear relationship between the a-Si TO peak full width of the half maximum Γ (cm⁻¹) and bond angle deviation $\Delta\theta$ (degree) in a-Si,⁴⁾

$$\Gamma/2 = 7.5 + 3 \Delta\theta. \quad (1)$$

The Γ values were determined by a curve fitting using Gaussian functions and $\Delta\theta$ was calculated based on Eq. (1). In order to compare the different ion species effects, the initial damage distributions during the Si⁺, P⁺, Ge⁺, and As⁺ ion implantations were calculated by Monte Carlo simulations using TRIM.⁵⁾ Figure 2 shows the calculated numbers of vacancies created by an ion per Å. Since the optical penetration depth in a-Si is ~100 nm at a wavelength of 488 nm, the ion dose was scaled using average displacements per target atom (DPA) calculated in the surface region with a depth of 100 nm. Figure 3 shows the changes in $\Gamma/2$ and $\Delta\theta$ as a function of each dose scaled by DPA. As can be seen in Fig. 3, larger DPA are necessary to obtain the same $\Delta\theta$ in the Si⁺ and P⁺ than the Ge⁺ and As⁺ implantation cases. This suggests that amorphization is controlled by the ion-beam-induced divacancy concentration⁶⁾ since more single vacancies are created along the ion paths and efficiency in generating the divacancies is higher in the latter cases. It is also seen that there exists a slight difference in the $\Delta\theta$ vs. DPA curve between the Si⁺ and P⁺, and Ge⁺ and As⁺ implantation cases. We believe that this is due to a chemical effect of P and As which enhance the growth of ion-induced damage probably through providing nucleation sites at the impurity location.

Figure 4 shows a typical example of the Raman spectra from 150 keV Si⁺ implanted Si(100) with a dose of 5×10^{15} cm⁻², before and after thermal annealing at 450 °C for 360 minutes. The TO peak half width $\Gamma/2$ decreases and the peak center shifts towards higher wavenumber. The surface a-Si layer thickness of the samples was ~200 nm as determined by cross-sectional TEM, and thus solid state epitaxial growth is negligible and the observed change in the Raman spectra can be attributed to the structural relaxation in a-Si.

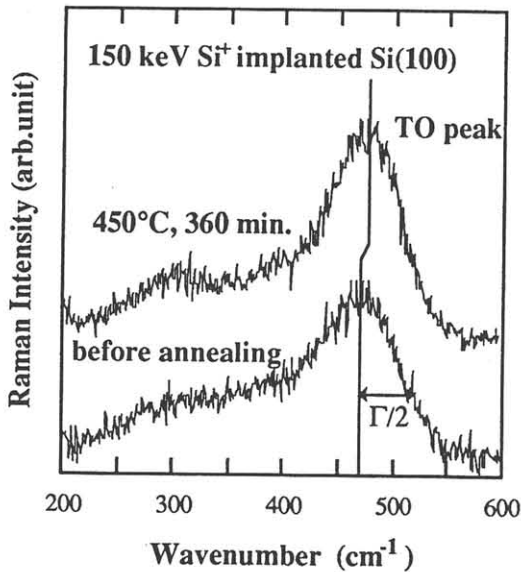


Fig. 4 Typical Raman spectra from Si(100) samples implanted with $5 \times 10^{15} \text{ cm}^{-2} \text{ Si}^+$ before and after annealing.

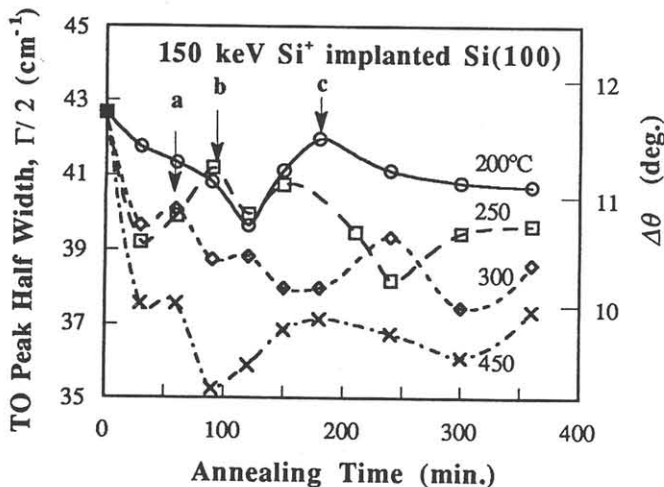


Fig. 5 Changes in $\Gamma/2$ and $\Delta\theta$ during isothermal annealing with various temperatures. The arrows a, b, and c represent the initial increase of $\Delta\theta$ for the annealing temperatures 300, 250, and 200 °C, respectively.

Based on the Raman measurements from the samples annealed at 200, 250, 300, and 450 °C, $\Gamma/2$ and $\Delta\theta$ were determined as a function of annealing time. These results are shown in Fig. 5. Although $\Delta\theta$ has been generally considered to decrease monotonically due to isothermal annealing,⁷⁾ $\Delta\theta$ obtained in the present experiments shows a slight increase after the initial decrease. This increase is observed more clearly and later in time as annealing temperature is lowered. Preliminary results of ESR measurements for the densities of dangling bonds in the same samples also showed similar changes to those described in Fig. 5.

We propose the following model for the results described above. Since the ion implantations were carried out at room temperature, the prepared a-Si layers may

include larger defects such as microvoids.²⁾ During thermal annealing, in addition to the bond angle relaxation in the continuous a-Si network, these microvoids will be dissociated into smaller defects such as dangling bonds. The former process contributes to the monotonic decrease of $\Delta\theta$ and the dangling bond density, while the latter increases not only the dangling bond density but also $\Delta\theta$.⁸⁾

4. CONCLUSION

We have investigated amorphization processes in Si^+ , P^+ , Ge^+ , and As^+ ion implanted c-Si as well as structural relaxation of a-Si during low-temperature (200–450°C) isothermal annealing using Raman spectroscopy combined with computer simulations of the initial ion-beam-induced damage profiles. The sharp c-Si Raman peak at 521 cm^{-1} decreased and the broad a-Si TO peak centered at $\sim 480 \text{ cm}^{-1}$ predominated as the implantation doses were increased. The bond angle deviation $\Delta\theta$ derived from the width of the a-Si TO peak was used to describe amorphous structure. The ion species effects were analyzed by scaling the ion dose using displacements per atom (DPA) calculated by Monte Carlo simulations. Larger DPA were necessary to obtain the same $\Delta\theta$ in the Si^+ and P^+ than Ge^+ and As^+ implantation cases suggesting that amorphization is controlled by divacancies generated by ion bombardment.

During isothermal annealing, $\Delta\theta$ was found not to decrease monotonically but to show a slight increase after the initial decrease. We have proposed that there exist microvoids in the initial a-Si layers and these microvoids are dissociated into smaller defects such as dangling bonds resulting in a increase of $\Delta\theta$.

ACKNOWLEDGEMENT

We would like to thank O. W. Holland of Oak Ridge National Laboratory and Y. Nakagawa of Applied Materials Japan for providing ion implanted samples. This work was partly supported by a Grant-In-Aid from the Ministry of Education, Science, and Culture.

REFERENCES

- 1) T. Motooka and O.W. Holland, Appl. Phys. Lett. **58**(1991) 2360.
- 2) T. Motooka, F. Kobayashi, P. Fons, T. Tokuyama, T. Suzuki, and N. Natsuaki, Jpn. J. Appl. Phys. **30**(1991) 3617.
- 3) P. A. Temple and C. E. Hathaway, Phys. Rev. **B7** (1973) 3685.
- 4) D. Beeman, R. Tsu, and M. F. Thorpe, Phys. Rev. **B32**(1985) 874.
- 5) J. P. Biersack, Nucl. Instrum. Methods **174**(1980) 257.
- 6) J. Linnros, R. G. Elliman, and W. L. Brown, J. Mater. Res. **3**(1988) 1208.
- 7) W. Sinke, T. Warabisako, M. Miyao, T. Tokuyama, S. Roorda, and F.W. Saris, Mat. Res. Soc. Symp. Proc. vol.100(1987) 549.
- 8) F. Kobayashi, T. Motooka, and T. Tokuyama, Proc. 14th Symp. on ISIA T'91, Tokyo(1991) 381.